J Solid State Electrochem (2014) 18:1077–1085
DOI 10.1007/s10008-013-2360-4

ORIGINAL PAPER

Properties of $LiMn_2O_4$ cathode in electrolyte based on ionic liquid with and without gamma-butyrolactone

Agnieszka Swiderska-Mocek

Received: 17 October 2013 / Revised: 2 December 2013 / Accepted: 9 December 2013 / Published online: 21 December 2013

Abstract $LiMn_2O_4$ was examined as a cathode material for the lithium-ion battery, working together with a room temperature ionic liquid electrolyte, obtained by dissolution of solid lithium bis(trifluoromethanesulphonyl)imide ($LiNTf_2$) in liquid N-methyl-N-propylpyrrolidinium bis (trifluoromethanesulphonyl) imide ($MePrPyrNTf_2$) with and without gamma-butyrolactone (GBL). The Li/$LiMn_2O_4$ cell was tested by cyclic voltammetry, galvanostatic charging/discharging, and with impedance spectroscopy. In the cyclic voltammograms for these electrolytes pairs of oxidation current peaks and reduction current peaks for the cathode are distinct, revealing typical characteristics of two-stage reversible-phase transformation of the spinel. The $LiMn_2O_4$ cathode showed good cyclability and Coulombic efficiency (126 mAh g^{-1} after 50 cycles) working together with 0.7 M $LiNTf_2$ in $MePrPyrNTf_2$+10 wt%. GBL ionic liquid electrolyte. At the C/7and C/5 rates, the $LiMn_2O_4$ showed stable capacities of 124 and 120 mAh g^{-1}, respectively. Scanning electron microscopy images of pristine electrodes and those taken after electrochemical cycling showed changes which may be interpreted as a result of solid electrolyte interphase formation. The 0.7 M $LiNTf_2$ in $MePrPyrNTf_2$ and 0.7 M $LiNTf_2$ in $MePrPyrNTf_2$+10 wt%. GBL electrolytes have a greater thermal stability range (no peak is observed below 230 °C).

Keywords Ionic liquid · Lithium-ion battery · Gamma-butyrolactone · $LiMn_2O_4$ cathode

A. Swiderska-Mocek (✉)
Faculty of Chemical Technology, Poznań University of Technology, 60-965 Poznań, Poland
e-mail: agnieszka.swiderska-mocek@put.poznan.pl

Introduction

In lithium or Li-ion batteries, the electrolyte reacts with electrodes by the formation of a passivation layer. This layer is usually called the solid electrolyte interphase (SEI) and protects them against further corrosion [1, 2]. The protective layer formed in such systems is responsible for the chemical stability of the anode and the cathode [3–7]. At high voltage differences (overcharging) or during contact with air (battery damage) the reaction of electrodes with the environment (solvent, moisture) may result in system ignition. Consequently, for safety reasons, all components of a Li-ion battery, including the electrolyte, should be characterized by non-flammability or negligible vapor pressure. A lithium salt ($LiPF_6$) solution in a mixture of linear and cyclic carbonates usually serves as the electrolyte for Li-ion batteries. However, these carbonates have low boiling points (below 150 °C) and low flashing points (below 30 °C). These are disadvantageous from the safety point of view. Instead of a salt solution in a volatile solvent, non-volatile molten salts may be applied as electrolytes. Salt liquids at room temperature, usually called room temperature ionic liquids or simply ionic liquids (IL), show considerable thermal stability, a wide liquid-phase range, non-flammability, negligible vapor pressure, and broad electrochemical stability [8–10]. Ionic liquids have been proposed as potential electrolytes for electrochemical capacitors and lithium-ion batteries, mainly due to their non-volatility and hence, non-flammability [8, 11–20]. Among ILs, those based on 1-ethyl-3-methyl-imidazolium [$EtMeIm^+$], N-alkyl-N-methylpiperidinium [$RMePip^+$], and N-alkyl-N-methylpyrrolidinium [$RMePyr^+$] cations and bis(trifluoromethanesulphonyl)imide anion [NTf_2^-] seem to be promising solvents for lithium salts. It is observed that these electrolytes were compatible with $LiCoO_2$, $LiFePO_4$, $Li[Li_{0.2}Mn_{0.54}Ni_{0.13}Co_{0.13}]O_2$ and $LiNi_{0.5}Mn_{1.5}O_4$ cathodes [12, 13, 18, 19, 21–23], as well as with graphite, $LaSi_2$/Si

and TiO_2 nanotube anodes [14, 20, 24, 25]. Recently, ionic liquids based on imidazolium and piperidinium cations with vinyl or allyl groups and [NTf_2^-] anion are of great interest as co-solvents for the Li-ion battery ($LiNi_{0.5}Mn_{1.5}O_4$ and $LiFePO_4$) [26, 27]. The evaluation of the cell $LiFePO_4$/Li with the mixed electrolyte based on N-allyl-N-methyl piperidinium bis(trifluoromethanesulfonyl)imide with $LiNTf_2$, and 30 wt% vinylene carbonate/dimethyl carbonate (1:1) shows good reversibility and cycle performances [27].

Gamma-butyrolactone (GBL) has a high boiling point, a low freezing point, a high flashing point, a high dielectric constant, and low viscosity [28, 29]. This low vapor pressure molecular solvent is a highly preferable co-solvent for lithium-ion batteries. However, GBL readily undergoes reductive decomposition on the surface of negative electrodes (graphite electrodes) and it forms a SEI characterized by considerable resistance [30]. Recently, GBL has been employed as a solvent for the lithium bis(oxalate)borate-based electrolyte [29, 31, 32]. Mass spectrometry was used to study the reductive decomposition of an electrolyte based on ethylene carbonate/dimethyl carbonate (EC/DMC), as well as the formation of the SEI in this electrolyte at the graphite electrode [33]. GBL, as an additive electrolyte, was observed to effectively diminish gas evolution in electrolyte solutions. GBL has also been mixed into the ionic liquid (1-butyl 3-methyl-imidazolium tetrafluoroborate, $BMIBF_4$) [34]. This mixture exhibits a greater thermal stability than the classical electrolyte. Most ionic liquids exhibit high viscosity and hence a relatively low conductivity. In order to decrease viscosity and increase conductivity an aprotic dipolar organic solvent may be added to IL. In these mixtures, the vapor pressure remains low and consequently, their flash point remains high [35].

Spinel-type lithium manganese oxide $LiMn_2O_4$ is one of the most frequently studied cathode materials for the use in Li-ion batteries. It has a specific capacity of ~120 mAh g^{-1} between 3.5 and 4.3 V and has no memory effects [36, 37]. However, the theoretical capacity of the spinel is 148 mAh g^{-1} [38]. In addition, $LiMn_2O_4$ is cheap and contains no heavy metals; hence, it is environmentally friendly. $LiMn_2O_4$ was examined in an ionic liquid based on trimethylhexylammonium [39, 40], N-methyl-N-propylpiperidinium [41], 1-cyanomethyl-3-methylimidazolium [42] cations and bis(trifluoromethanesulphonyl)imide anion. The $LiMn_2O_4$ cathode in the ionic liquid was observed to exhibit thermal stability. It is a promising aspect for the improvement of battery cell safety. A phosphazenic compound triethoxyphosphazen-N-phosphoryldiethylester [43] and a binary mixture of triethylphosphate and EC [41] were also studied as non-flammable electrolyte additives for Li-ion cells with the $LiMn_2O_4$ cathode.

The general aim of this paper was to study the $LiMn_2O_4$ cathode in ionic liquid with and without GBL as an additive. This organic solvent has been mixed to N-methyl-N-propylpyrrolidinium bis(trifluoromethanesulphonyl)imide ($MePrPyrNTf_2$) as ionic liquid in the presence of lithium bis(trifluoromethanesulphonyl)imide ($LiNTf_2$).

Experimental

Materials

$LiMn_2O_4$ powder (Aldrich), graphite KS-15 (G) (Lonza), poly(vinylidene fluoride) (PVdF, Fluka), GBL (Aldrich), lithium foil (0.75-mm thick, Aldrich) and lithium bis(trifluoromethanesulphonyl)imide ($LiNTf_2$, Fluka) were used as received. N-methyl-N-propylpyrrolidinium bis(trifluoromethanesulphonyl)imide ($MePrPyrNTf_2$) was prepared according to the literature [20]. *N*-methyl-*N*-propylpyrrolidinium bromide (MePrPyrBr) was obtained from N-methylpyrrolidinium (Aldrich) and bromopropane (Aldrich) in acetone. After decanting acetone the solid phase was dissolved in 2-propanol (P.O.Ch., Poland) and after the addition of tetrahydrofurane (P.O.Ch., Poland) white crystals of MePrPyrBr were precipitated. $MePrPyrNTf_2$ was obtained from MePrPyrBr by metathesis with lithium bis(trifluoromethanesulfonyl)imide in an aqueous medium. The ionic liquid was dried by vacuum evaporation at 50 °C for 10 h and kept over A3 molecular sieves. Liquid electrolyte (0.7 M $LiNTf_2$ in $MePrPyrNTf_2$) was obtained by dissolution of solid $LiNTf_2$ salt in liquid $MPPyrNTf_2$. Electrolyte containing GBL (10 % wt.) was prepared in a dry argon atmosphere in a glove box. Positive electrodes were prepared by casting a slurry of the $LiMn_2O_4$, graphite (G) and PVdF (a 85:5:10 ratio) in N-methyl-2-pyrrolidone (NMP, Fluka) on a golden current collector (radius 12 mm). The layer of the cathode was formed by vacuum evaporation of the solvent (NMP) at 120 °C. The electrode typically contained 1.5–2.5 mg of $LiMn_2O_4$.

Measurements

The $LiMn_2O_4$/electrolyte/Li cells were assembled in a dry argon atmosphere in a glove box. The $LiMn_2O_4$ electrode and a round-shaped lithium electrode was cut off from the metallic-lithium foil (surface of 1 cm^2), and separated by a glass micro-fiber GF/A separator (Whatman) soaked with the electrolyte placed in an adapted 0.5 Swagelok® connecting tube. The cycling measurements were taken with the use of the ATLAS 0461 MBI multichannel electrochemical system (Atlas-Solich, Poland) at different current densities (C/10–C/2). Constant current charging/discharging cycles were conducted between 3.2 and 4.3 V versus the lithium reference. Cyclic voltammetry, as well as electrochemical impedance spectroscopy (EIS), were performed with the use of the

G750 Potentiostat/Galvanostat Measurements System (Gamry, USA). Impedance spectra were obtained using a frequency response analyzer at a frequency range of 100 kHz–10 mHz, at the open circuit potential and amplitude of 10 mV. Conductivity of electrolytes was measured in a two electrode (Pt) thermostated conductometric glass cell with the constant of 4.80 cm^{-1}. During conductivity measurements of electrolyte impedance were recorded between 1 Hz and 10 kHz at the amplitude of 10 mV. Density of electrolytes was measured with an Anton Paar DMA 35-N meter. Flash points of electrolytes with and without gamma-butyrolactone were measured with the use of an open-cup home-made apparatus, based on the Cleveland instrument, with a 1.5-ml cup. The apparatus was scaled with a number of compounds with known flash points. The cup was heated electrically through a sand bath and the temperature was measured with the M-3850 Metex (Korea) digital thermometer. The thermal behavior of electrolytes in the temperature range of 20–280 °C was studied by differential scanning calorimeter (DSC). A differential scanning calorimeter model DSC XP-10 by Thass GmbH was used. Scanning electron microscopy (SEM) of electrodes was performed with the Tescan Vega 5153 apparatus.

Results and discussion

Electrolyte composition, conductivity, and density

The specific conductivity of the neat ionic liquid $MePrPyrNTf_2$ was 1.4 mS cm^{-1} at 25 °C [44]. Ionic liquid electrolyte was obtained by dissolution of solid $LiNTf_2$ in liquid $MePrPyrNTf_2$ (0.7 M solution of $LiNTf_2$ in $MePrPyrNTf_2$). The resulting ternary $LiNTf_2$ - $MePrPyrNTf_2$ ionic liquid had a density of ca. 1.479 g cm^{-3} and the composition of $[Li^+]_{0.09}[MePrPyr^+]_{0.41}[NTf_2^-]_{0.50}$ [20]. At higher $LiNTf_2$ concentrations, a crystalline solid phase was formed. After dissolving lithium salt in an ionic liquid conductivity has increased slightly (1.6 mS cm^{-1} for 0.7 M $LiNTf_2$ in $MePrPyrNTf_2$). On the other hand, an addition of relatively small amounts of GBL resulted in an increase of conductivity to ca. 3.6 mS cm^{-1} for 0.7 M $LiNTf_2$ in $MePrPyrNTf_2$ (90 wt%) + GBL (10 wt%).

Cyclic voltammetry

Cyclic voltammograms (CV) of cathode $LiMn_2O_4$ in ionic liquid ($MePrPyrNTf_2$) with and without an addition of GBL are shown in Fig. 1. Two pairs of oxidation current peaks and reduction current peaks for the cathode are distinct, revealing typical characteristics of two-stage reversible-phase transformation of the spinel $LiMn_2O_4$. Two pairs of separated redox peaks show that lithium ions are extracted and inserted

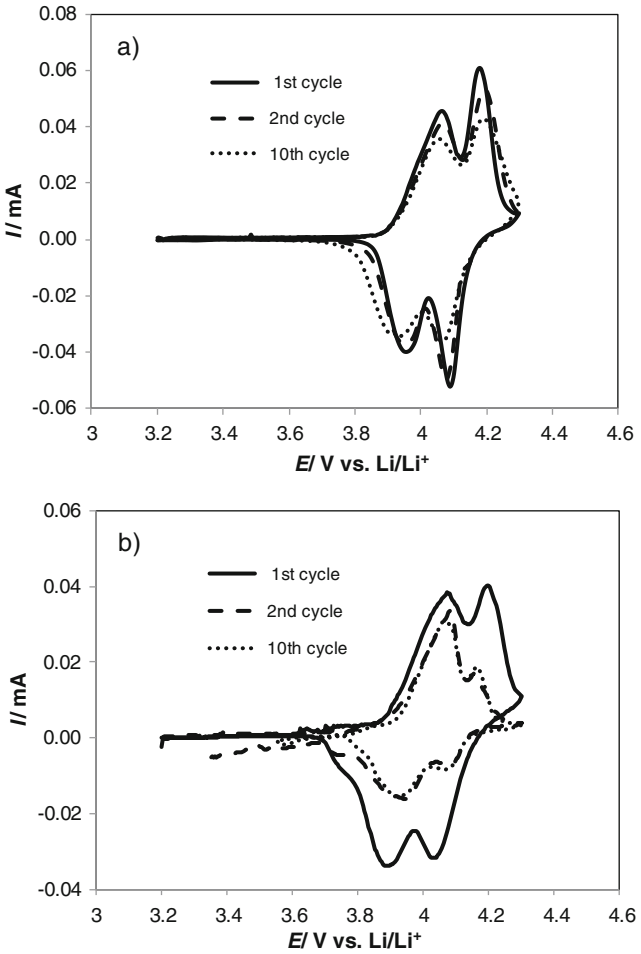

Fig. 1 Cyclic voltammograms of spinel $LiMn_2O_4$ in (**a**) 0.7 M $LiNTf_2$ in $MePrPyrNTf_2$+10 % wt. GBL and (**b**) 0.7 M $LiNTf_2$ in $MePrPyrNTf_2$. Scan rate: 0.01 mV s^{-1}

from/into the spinel phase by a two-step process [45, 46]. Figure 1a shows the cyclic voltammogram of a $LiMn_2O_4$ particle in 0.7 M $LiNTf_2$ in $MePrPyrNTf_2$+10 wt% GBL. Two peaks are clearly observed at 4.00 and 4.15 V in both anodic and cathodic scans. The redox peaks of the $LiMn_2O_4$ electrode are sharp with a well-defined splitting. The peak currents and the peak potentials did not change significantly during cycling. In electrolyte with GBL, the $LiMn_2O_4$ particles showed excellent cycle stability. While in the case of the $MePrPyrNTf_2$ ionic liquid peaks are less sharp and reversibility of the insertion/extraction process is poorly observed (Fig. 1b). The peak heights gradually decreased during cycling. It seems that the electrolyte (0.7 M $LiNTf_2$ in $MePrPyrNTf_2$) not is stable up to 4.3 V (Li^+ versus Li) against oxidation for $LiMn_2O_4$ electrode.

Galvanostatic charging/discharging

Charge–discharge curves of the $LiMn_2O_4$/Li half cell using the electrolyte with and without the additive are shown in

Fig. 2. It can be seen that the charge/discharge curves of $LiMn_2O_4$ electrode exhibit two potential plateaus, in accord with the results of the CV curve in Fig. 1. Figure 2a presents charging/discharging curves, for the spinel electrode working with 0.7 M $LiNTf_2$ in $MePrPyrNTf_2$+10 wt% GBL. The addition of GBL (10 wt%.) improves both the charging and discharging capacities in subsequent cycles, in comparison to the ionic liquid ($MePrPyrNTf_2$) without any additive (Fig. 2b). After the first cycle, the discharge capacity of the spinel was ca. 144 mAh g^{-1}, close to its theoretical maximum value. During the next cycles, the capacity of the electrode decreases gradually to stabilize at ca. 126 mAh g^{-1} after 50 cycles. The improvement is probably due to the ability of the additive (GBL in $MePrPyrNTf_2$) to form SEI on the electrodes surface. In the case of the spinel electrode working with the neat ionic liquid, the capacity of the charging (q_{ch}) and discharging (q_{dis}) processes at the first cycle was 157 and 121 mAh g^{-1}, respectively (Fig. 2b). However, the capacity of the electrode further decreased during the cycling. The electrode showed ca. 60 % of the theoretical charge and discharge capacities (80 mAh g^{-1}) after 50 cycles, at the charge/discharge current of 14 mA g^{-1} (C/10). In 0.7 M $LiNTf_2$ in $MePrPyrNTf_2$ electrolyte, the $LiMn_2O_4$ spinel shows little stability. A comparison of the discharge capacity and the Coulombic efficiency for the spinel electrode working together with the neat ionic liquid, as well as the additive is shown in Fig. 3. The Coulombic efficiency, proportional to the q_{dis}/q_{ch} ratio, increased during the cycling to reach almost 100 % after the 15th cycle for 0.7 M $LiNTf_2$ in $MePrPyrNTf_2$+10 wt% GBL (Fig. 3b). The discharge capacity of the $LiMn_2O_4$|electrolyte|Li cell depends on the current rates (Fig. 4). The cells could work relatively efficiently over many cycles at higher rates. In the case of the ionic liquid with the additive (0.7 M $LiNTf_2$ in $MePrPyrNTf_2$+10 wt% GBL) at high capacity (ca. 120 mAh g^{-1}) was obtained at the C/7and C/5 rates. After 20 electrochemical cycles, no capacity loss was observed, showing a satisfactory cycle ability of the $LiMn_2O_4$ cathode. However, at the C/2 rate the discharge capacity dropped to 94 mAh g^{-1}. On the other hand, for 0.7 M $LiNTf_2$ in $MePrPyrNTf_2$, the charging/discharging rate of C/7 led to the electrode capacity of ca. 72 mAh g^{-1} after 20 cycles. A further capacity fading was observed during the 20

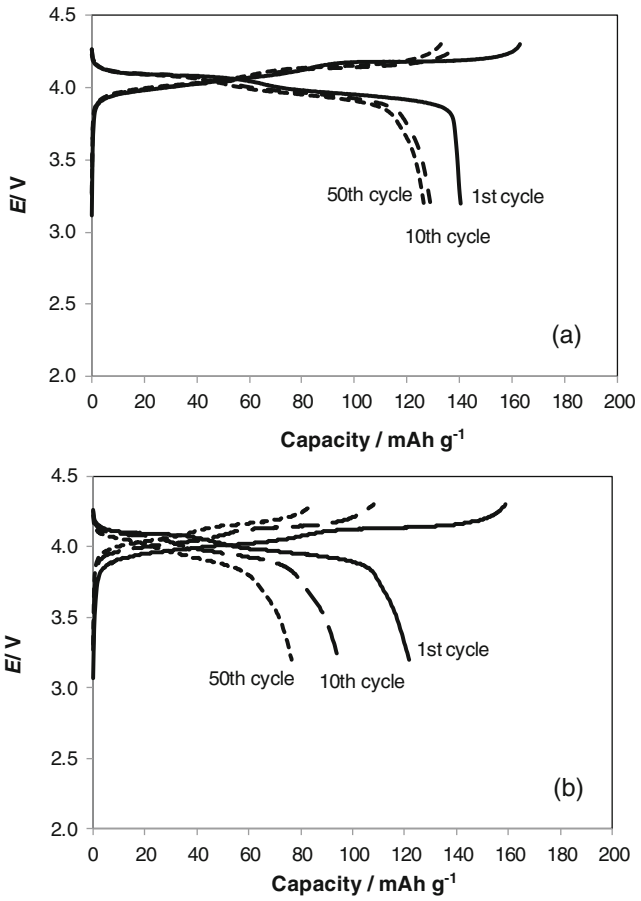

Fig. 2 Charging/discharging of (**a**) $LiMn_2O_4$|0.7 M $LiNTf_2$ in $MePrPyrNTf_2$+10 % wt. GBL|Li and (**b**) $LiMn_2O_4$|0.7 M $LiNTf_2$ in $MePrPyrNTf_2$ |Li cells. Spinel mass in the cathode: (**a**) 1.9 mg and (**b**) 2.0 mg. Current: 14 mA g^{-1} (C/10)

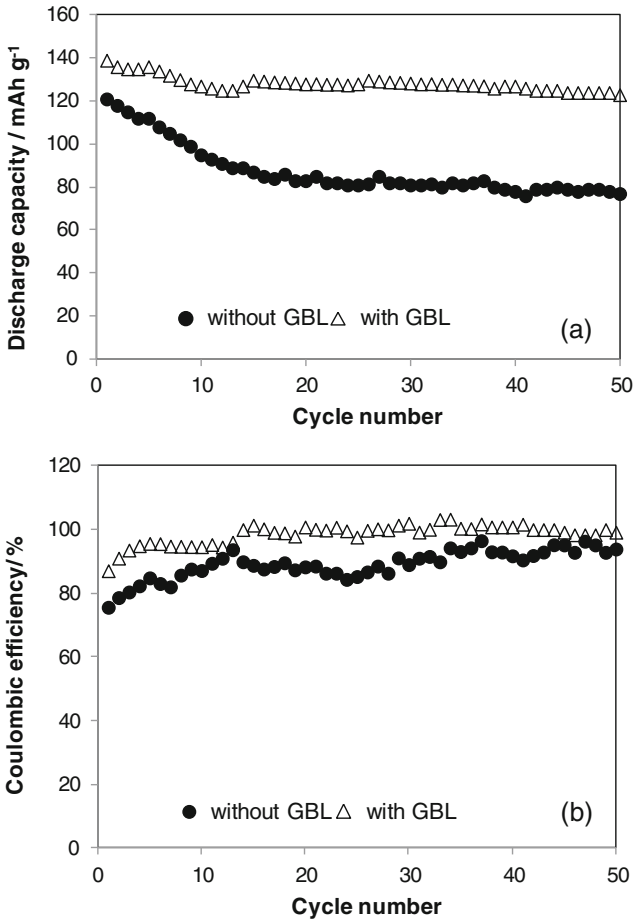

Fig. 3 Discharging capacity (**a**) and Coulombic efficiency (**b**) of the $LiMn_2O_4$|electrolyte|Li cell. Electrolytes: (*black circles*) 0.7 M $LiNTf_2$ in $MePrPyrNTf_2$, and (*white triangles*) 0.7 M $LiNTf_2$ in $MePrPyrNTf_2$+ 10 wt% GBL. Current: 14 mA g^{-1} (C/10)

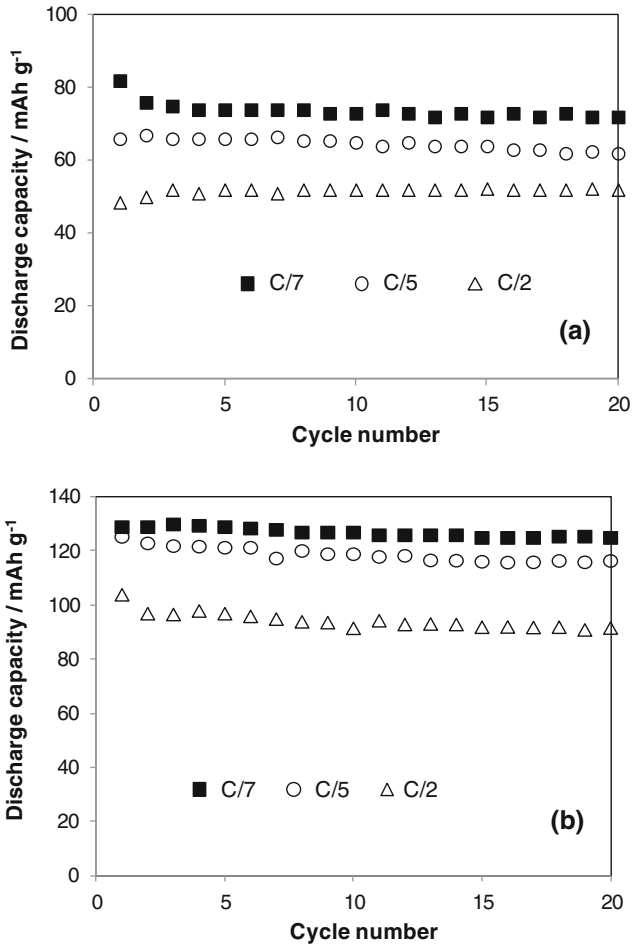

Fig. 4 Discharging capacity of $LiMn_2O_4$|electrolyte|Li cells at various discharging rates. Electrolytes: (**a**) 0.7 M $LiNTf_2$ in $MePrPyrNTf_2$ and (**b**) 0.7 M $LiNTf_2$ in $MePrPyrNTf_2$+10 wt% GBL

cycles at the C/5 and C/2 discharge rates. A comparable capacity (ca. 120 mAh g^{-1}) for the $LiNi_{0.5}Mn_{1.5}O_4$ cathode was obtained using a mixture of the classical 1 M $LiPF_6$ solution in 50 wt% EC+50 wt% diethyl carbonate and an ionic liquid (1-ethyl-1-methylpiperidinium bis(trifluoromethanesulfonyl)imide) electrolyte (1:1) [23]. In the case of a mixed spinel cathode, its theoretical capacity is much higher than that of the $LiMn_2O_4$ cathode. The Li/Li[$Li_{0.2}Mn_{0.54}Ni_{0.13}Co_{0.13}$]$O_2$ system with an ionic liquid as an additive (N-butyl-N-methylpyrrolidinium bis(trifluoromethanesulfonyl)imide) was studied [22]. With 60 % $BuMePyrNTf_2$-added electrolyte, Li[$Li_{0.2}Mn_{0.54}Ni_{0.13}Co_{0.13}$]$O_2$ shows a better cycling stability with a capacity retention of 84.4 % after 150 cycles than that in IL free electrolyte. The discharge capacity of the cell with pure IL electrolyte decreases rapidly to only 35 mAh g^{-1} at 1 C.

Impedance study

Anodes characterized by a low potential, such as lithium metal or lithiated graphite, react spontaneously with the electrolyte. Therefore, these electrodes require the formation of a protective coating. Use of suitable electrolytes or electrolyte additives is an effective method for the improvement of the cycle-life of Li-ion batteries [40, 42, 43]. Compatibility of the mixed electrolyte of two ionic liquids ($CmMeImNTf_2$ with the cyano group and $EtMeImNTf_2$) with $LiMn_2O_4$, $LiFePO_4$ and graphite was studied. In the case of $LiMn_2O_4$, the capacity in the mixed ionic liquids is recovered by subsequent cycling [42]. The additive enables SEI formation on the surface of both the anode and cathode [3, 41, 47]. The electrochemical reaction of the electrolyte additive (e.g., vinylene carbonate) at electrode materials may result in the formation of a coating and a modification of the electrode surface. The type of additive also affects the chemical structure of the electrolyte/electrode interface, which in turn affects the efficient migration of lithium ions and hence the performance of the cell. The passivation of both the $LiMn_2O_4$ cathode and the lithium anode was observed using impedance spectroscopy. The impedance spectra were recorded in two electrode cell using Li counter. At the time, the EIS results also include impedance of the lithium (anode) interface. Nyquist plots for $LiMn_2O_4$|Li cells with different electrolyte compositions are shown in Figs. 5, 6, and 7. Typically, spectra taken immediately after the cell assembling consist of a semicircle followed by a straight line (Fig. 5). However, after 20 galvanostatic charging/discharging (C/7) cycles, two semicircles can be seen at the high-frequency region (Figs. 6 and 7). The first semicircle reflects the formation of the SEI layer and the second the charge transfer process, while the line at the low-frequency region represents the diffusion process (of Li^+ in the electrolyte and SEI, or Li in solid electrodes) [48]. On the other hand, the impedance plots consisting of two semicircles may also be attributed to the anode/electrolyte interface (the high-frequency semicircle) and to the cathode/electrolyte interface (the low-frequency semicircle) [41]. The equivalent circuit used for impedance spectra deconvolution (Fig. 8) consisted of two *RC* elements describing resistance of SEI (R_{SEI}) and resistance of the charge transfer reaction (R_{ct}), in series with electrolyte resistance R_{el} and diffusion impedance represented by the Warburg element (Z_W). The SEI resistance of the $LiMn_2O_4$|0.7 M $LiNTf_2$ in $MePrPyrNTf_2$|Li system was R_{SEI}=220 Ω, while the charge transfer resistance was R_{ct}= 135 Ω (Fig. 6). However, after 20 galvanostatic charging/discharging the R_{SEI} and R_{ct} increased to values 250 and 642 Ω, respectively. The higher charge transfer resistance (R_{ct}) of the $LiMn_2O_4$|0.7 M $LiNTf_2$ in $MePrPyrNTf_2$|Li cell signifies the more capacity loss in the high charge/discharge rate, which is in good agreement with the C-rate capacity data. On the other hand, in the case of the $LiMn_2O_4$|0.7 M $LiNTf_2$ in $MePrPyrNTf_2$+ 10 wt% GBL|Li system a much smaller increase of resistance was observed (Fig. 7). After 20 galvanostatic charging/discharging, the charge transfer resistance and SEI resistance were 178 and 126 Ω, respectively. The

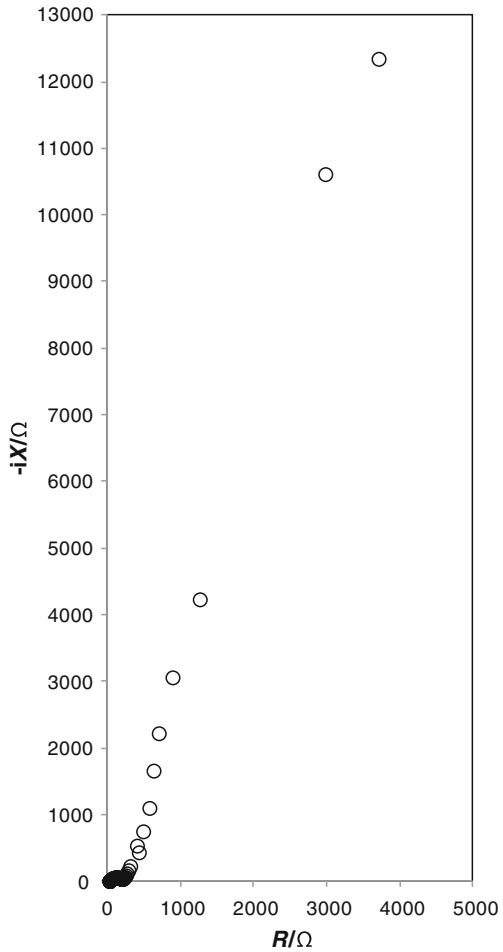

Fig. 5 Impedance spectroscopy of $LiMn_2O_4$|0.7 M $LiNTf_2$ in $MePrPyrNTf_2$|Li system recorded after cell assembling (measured E= 3.25 V vs. Li/Li^+). Frequency range 10^5–10^{-2} Hz

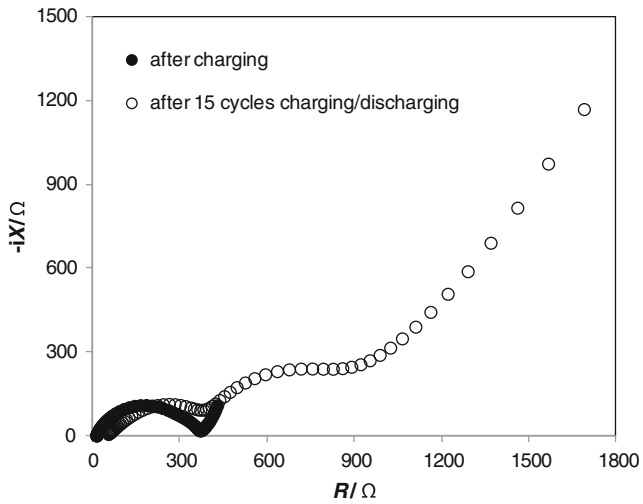

Fig. 6 Impedance spectroscopy of $LiMn_2O_4$|0.7 M $LiNTf_2$ in $MePrPyrNTf_2$|Li system (*black circles*) after charging (measured E= 4.25 V vs. Li/Li^+) and (*white circles*) after 20 cycles of galvanostatic charging/discharging (C/7) (measured E=4.20 V vs. Li/Li^+). Frequency range 10^5–10^{-2} Hz

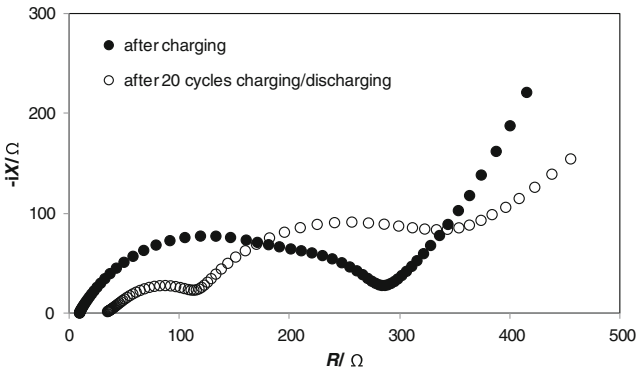

Fig. 7 Impedance spectroscopy of $LiMn_2O_4$|0.7 M $LiNTf_2$ in $MePrPyrNTf_2$+10 wt%. GBL |Li system (*black circles*) after charging (measured E=4.26 V vs. Li/Li^+) and (*white circles*) after 20 cycles of galvanostatic charging/discharging (C/7) (measured E=4.21 V vs. Li/Li^+). Frequency range 10^5–10^{-2} Hz

electrolyte additive and the electrochemical process are necessary for the formation of the protective SEI coating in the systems under study. There is some difference in the chemistry at the interface, the so-called SEI formation, depending on the electrolyte composition. Such a change in the interfacial property would reduce the impedance and then improve the charge–discharge performance of the cell. These results show that GBL is a safe and effective component for the $MePrPyrNTf_2$ ionic liquid, improving the electrochemical performance of the $LiMn_2O_4$|Li system. Figure 9 shows SEM images of a pristine electrode and those after electrochemical cycling with different electrolytes. The pristine cathode (Fig. 9a and b) is composed of an agglomerated structure morphology and it is porous. However, after electrochemical cycling in 0.7 M $LiNTf_2$ in $MePrPyrNTf_2$ and 0.7 M $LiNTf_2$ in $MePrPyrNTf_2$+10 wt% GBL the cathode is covered with small aggregates. This 'micro-roughness' may indicate the formation of a SEI layer [3].

Electrolyte flammability and thermal stability

For safety reasons, it is important to use non-volatile electrolytes in lithium-ion cells. Many ionic liquids, due to strong ion-ion interactions, are characterized by negligible vapor pressure and are completely non-volatile. Therefore, the flash

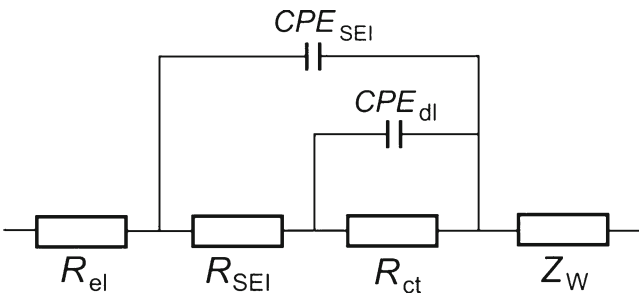

Fig. 8 An equivalent circuit representing the electrode/electrolyte system

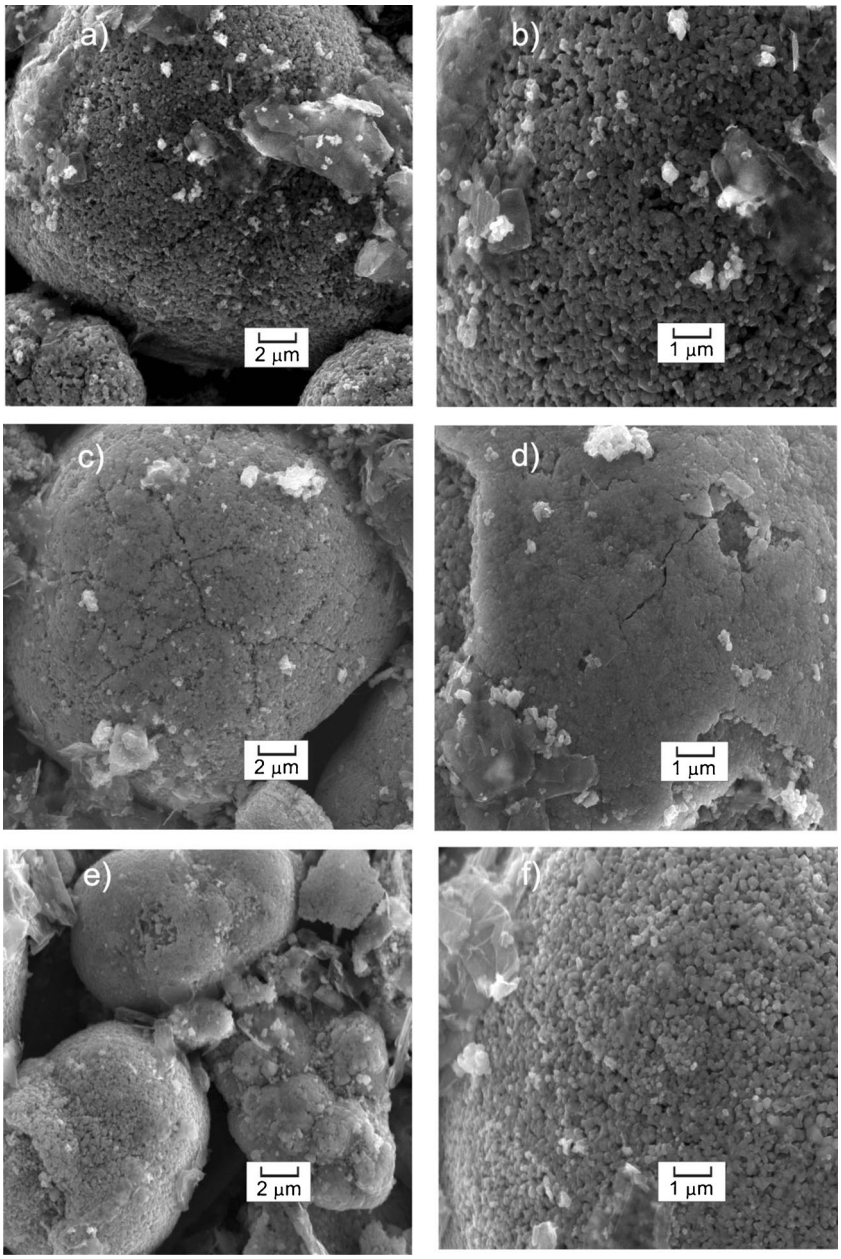

Fig. 9 SEM images of the $LiMn_2O_4$ cathode: pristine electrode (**a** and **b**), after 20 charge/discharge cycles (**c**, **d**, **e**, **f**). Electrolyte: 0.7 M $LiNTf_2$ in $MePrPyrNTf_2$ (**c**, **d**) and 0.7 M $LiNTf_2$ in $MePrPyrNTf_2$+ 10 wt% GBL (**e**, **f**). Magnification: 5000 x (**a**, **c**, **e**) and 10000 x (**b**, **d**, **f**)

point of electrolytes was determined as described in the experimental section. The results are shown in Table 1. Ionic liquid with lithium salt (0.7 M $LiNTf_2$ in $MePrPyrNTf_2$) displays flash points above 270 °C. The addition of gamma-butyrolactone (with the flash point of 101 °C) to the electrolyte decreases its flash point. On the other hand, during SEI formation the additive (GBL) is converted into a component of the interface. Consequently, the amount of the volatile compound decreases to a low value, increasing the flash point of the electrolyte. The flash points of 0.7 M $LiNTf_2$ in $MePrPyrNTf_2$+10 wt% GBL was 152 °C. This value is higher than that observed for a conventional 1 M $LiPF_6$ solution in EC/DMC (1:1) (35 °C) [49]. In addition, if these electrolytes are in contact with the cathode ($LiMn_2O_4$), the flash point does not change.

Table 1 A comparison of flash points

Electrolyte	Flash point (°C)
0.7 M $LiNTf_2$ in $MePrPyrNTf_2$	>270
0.7 M $LiNTf_2$ in $MePrPyrNTf_2$+10 wt% GBL	152
$LiMn_2O_4$ (solid)+0.7 M $LiNTf_2$ in $MePrPyrNTf_2$	>270
$LiMn_2O_4$ (solid)+0.7 M $LiNTf_2$ in $MePrPyrNTf_2$+ 10 wt% GBL	150

All these findings suggest that the replacement of a classical electrolyte in molecular liquids (cyclic carbonates) by an electrolyte based on an ionic liquid or ionic liquid with additives brings about a high increase in cathode/electrolyte non-flammability. If an additive can function both as a fire-retardant and protect against overcharge, it would provide more reliable protection for Li-ion batteries at extended storage and under extreme working conditions [50]. DSC thermograms of electrolyte-based ionic liquid are presented in Fig. 10. The thermograms of 0.7 M $LiNTf_2$ in $MePrPyrNTf_2$ and 0.7 M $LiNTf_2$ in $MePrPyrNTf_2$+10 % wt. GBL electrolytes show a greater thermal stability range, with no peak observed below 230 °C. The 0.7 M $LiNTf_2$ in $MePrPyrNTf_2$ electrolyte was very stable up to 280 °C. Here, we can see that the beneficial effects of these electrolytes are due to the good thermal stability of ionic liquid ($MePrPyrNTf_2$). Decomposition of the ionic liquids is observed just above 400 °C (e.g., $EtMeImNTf_2$ decomposed between 440 and 480 °C [51]). However, GBL has a high boiling point (207 °C at the atmospheric pressure) [28], but it does not exceed 230 °C. GBL molecules in 0.7 M $LiNTf_2$ in $MePrPyrNTf_2$ are probably involved in ion salvation and hence they are non-volatile. This experiment reveals the enhanced stability of organic solvents such as GBL when mixed with very stable ionic liquid.

Conclusions

1. During charging/discharging tests, the $LiMn_2O_4$ cathode working together with the 0.7 M $LiNTf_2$ in $MePrPyrNTf_2$ electrolyte loses its capacity during cycling and stabilizes at ca. 80 mAh g^{-1} after 50 cycles. The addition of GBL to the electrolyte (0.7 M $LiNTf_2$ in $MePrPyrNTf_2$+10 wt% GBL) considerably increases the cathode capacity. The $LiMn_2O_4$ cathode showed good cyclability and Coulombic efficiency (126 mAh g^{-1} after 50 cycles) working together with 0.7 M $LiNTf_2$ in $MePrPyrNTf_2$+10 wt% GBL ionic liquid electrolyte. After 20 electrochemical cycles, no capacity loss was observed (ca. 120 mAh g^{-1}at the C/7and C/5 rates), showing a satisfactory cycle ability of the $LiMn_2O_4$ cathode.
2. In the cyclic voltammograms pairs of oxidation current peaks and reduction current peaks for the cathode are distinct, revealing typical characteristics of two-stage reversible-phase transformation of the $LiMn_2O_4$ spinel. Two peaks are clearly observed at 4.00 and 4.15 V in both anodic and cathodic scans.
3. The pristine cathode (SEM images) is composed of agglomerated structure morphology and it is porous. However, after electrochemical cycling in 0.7 M $LiNTf_2$ in $MePrPyrNTf_2$ and 0.7 M $LiNTf_2$ in $MePrPyrNTf_2$+ 10 wt% GBL, the cathode is covered with small aggregates.
4. The 0.7 M $LiNTf_2$ in $MePrPyrNTf_2$ and 0.7 M $LiNTf_2$ in $MePrPyrNTf_2$+10 wt% GBL electrolytes have a greater thermal stability range, with no peak observed below 230 °C. The flash point of 0.7 M $LiNTf_2$ in $MePrPyrNTf_2$ was 270 °C, which makes them practically non-flammable.
5. These results (galvanostatic charging/discharging, EIS and SEM) showed that GBL is a safe and effective component for the $MePrPyrNTf_2$ ionic liquid, improving the electrochemical performance of the $LiMn_2O_4$|Li system.

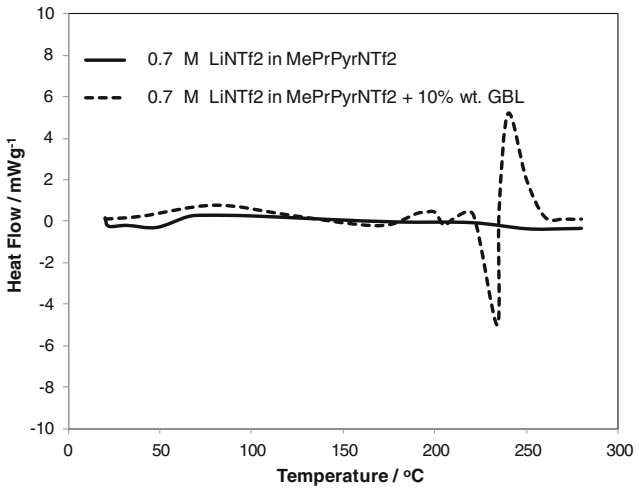

Fig. 10 DSC thermogram of 0.7 M $LiNTf_2$ in $MePrPyrNTf_2$ and 0.7 M $LiNTf_2$ in $MePrPyrNTf_2$+10 wt% GBL electrolytes at a rate of 10 °C min^{-1}

Acknowledgments The support of the 31-254/2013 DS-PB grant is gratefully acknowledged.

References

1. Wakihara M, Yamamoto O (1998) Lithium ion batteries. Wiley-VCH, Tokyo
2. Scrosati B, Garche J (2010) J Power Sources 195:2419–2430
3. Aurbach D (2000) J Power Sources 89:206–218
4. Aurbach D (2002) In: van Schalkwijk WA, Scrosati B (eds) Advances in lithium-ion batteries. New York, Kluwer
5. Edström K, Herstedt M, Abraham DP (2006) J Power Sources 153: 380–384
6. Aurbach D, Markovsky B, Salitra G, Markevich E, Taluossef Y, Koltypin M, Nazar L, Ellis B, Kovacheva D (2007) J Power Sources 165:491–499
7. Zhang SS (2006) J Power Sources 162:1379–1394
8. Galiński M, Lewandowski A, Stępniak I (2006) Electrochim Acta 51:5567–5580
9. Hu Y, Li H, Huang X, Chen L (2004) Electrochem Commun 6:28–32

10. Ngo HL, LeCompte K, Hargens L, McEwen AB (2000) Thermochim Acta 357–358:97–102
11. Fernicola A, Scrosati B, Ohno H (2006) Ionics 12:95–102
12. Holzapfel M, Jost C, Novak P (2004) Chem Commun 2098–2099
13. Seki S, Kobayashi Y, Miyashiro H, Ohno Y, Usami A, Mita Y, Kihira N, Watanabe M, Terada N (2006) J Phys Chem B 110:10228–10230
14. Holzapfel M, Jost C, Prodi-Schwab A, Krumeich F, Wursig A, Buqa H, Novak P (2005) Carbon 43:1488–1498
15. Lewandowski A, Swiderska-Mocek A (2007) J Power Sources 171: 938–943
16. Guerfi A, Duchesne S, Kobayashi Y, Vijh A, Zaghib K (2008) J Power Sources 175:866–873
17. Webber A, Blomgren GE (2002) In: van Schalkwijk WA, Scrosati B (eds) Advances in lithium-ion batteries. New York, Kluwer
18. Guerfi A, Dontigny M, Charest P, Petitclerc M, Lagace M, Vijh A, Zaghib K (2010) J Power Sources 195:845–852
19. Matsumoto H, Sakaebe H, Tatsumi K, Kikuta M, Ishiko E, Kono M (2006) J Power Sources 160:1308–1313
20. Lewandowski A, Swiderska-Mocek A (2009) J Power Sources 194: 502–507
21. Wang M, Shan Z, Tian J, Yang K, Liu X, Liu H, Zhu K (2013) Electrochim Acta 95:301–307
22. Zheng J, Zhu D, Yang Y, Fung Y (2012) Electrochim Acta 59:14–22
23. Kim K, Cho YH, Shin HC (2013) J Power Sources 225:113–118
24. Usui H, Shimizu M, Sakaguchi H (2013) J Power Sources 235:29–35
25. Ivanov S, Cheng L, Wulfmeier H, Albrecht D, Fritze H, Bund A (2013) Electrochim Acta 104:228–235
26. Wang ZN, Cai YJ, Wang ZH, Chen SM, Lu XM, Zhang SJ (2013) J Solid State Electrochem 17:2839–2848
27. Zhou JH, Li CH, Yang BB (2013) Adv Mater Res 750–752:1194–1198
28. Kinoshita SC, Kotato M, Sakata Y, Ue M, Watanabe Y, Morimoto H, Tobishima SI (2008) J Power Sources 183:755–760
29. Huang JY, Liu XJ, Kang XL, Yu ZX, Xu TT, Qiu WH (2009) J Power Sources 189:458–461
30. Aurbach D (1989) J Electrochem Soc 136:1606–1610
31. Azeez F, Fedkiw PS (2010) J Power Sources 195:7627–7633
32. Ping P, Wang Q, Sun J, Feng X, Chen C (2011) J Power Sources 196: 776–783
33. Lanz M, Novak P (2001) J Power Sources 102:277–282
34. Chagnes A, Diaw M, Carre B, Willmann P, Lemordant D (2005) J Power Sources 145:82–88
35. Chagnes A, Carre B, Willmann P, Lemordant D (2001) Electrochim Acta 46:1783–1791
36. Gabrisch H, Ozawa Y, Yazami R (2006) Electrochim Acta 52:1499–1506
37. Zhang SS, Jow TR (2002) J Power Sources 109:172–177
38. Xia Y, Yoshio M (1997) J Power Sources 66:129–133
39. Zheng H, Zhang H, Fu Y, Abe T, Ogumi Z (2005) J Phys Chem B 109:13676–13684
40. Zheng H, Li B, Fu Y, Abe T, Ogumi Z (2006) Electrochim Acta 52: 1556–1562
41. Lalia BS, Yoshimoto N, Egashira M, Morita M (2010) J Power Sources 195:7426–7431
42. Egashira M, Kanetomo A, Yoshimoto N, Morita M (2010) Electrochemistry 78:370–374
43. Wu B, Pei F, Wu Y, Mao R, Ai X, Yang H, Cao Y (2013) J Power Sources 227:106–110
44. MacFarlane DR, Meakin P, Sun J, Amini N, Forsyth M (1999) J Phys Chem B 103:4164–4170
45. Ding Y, Xie J, Cao G, Zhu T, Yu H, Zhao X (2011) Adv Funct Mater 21:348–355
46. Dokko K, Horikoshi S, Itoh T, Nishizawa M, Mohamedi M, Uchida I (2000) J Power Sources 90:109–115
47. Zhou WJ, He BL, Li HL (2008) Mater Res Bull 43:2285–2294
48. Wang YZ, Shao X, Xu HY, Xie M, Deng SX, Wang H, Liu JB, Yan H (2013) J Power Sources 226:140–146
49. Lewandowski A, Acznik I, Swiderska-Mocek A (2010) J Appl Electrochem 40:1619–1624
50. Feng JK, Cao YL, Ai XP, Yang HX (2008) Electrochim Acta 53: 8265–8268
51. Bonhôte P, Dias AP, Papageorgiou N, Kalyanasundaram K, Grätzel M (1996) Inorg Chem 35:1168–1178